Event report 24-29 October 2021

Silvia Puca[1], Alessandra Mascitelli[1,2], Marco Petracca[1], Alexander Toniazzo[1], Simone Gabellani[3], Martina Lagasio[3], Vincenzo Mazzarella[3], Luca Pulvirenti[3], Luca Brocca[4], David Fairbairn[5], Giulia Panegrossi[2] and the H SAF TEAM

[1] National Civil Protection Department (DPC), Rome, Italy
[2] Institute of Atmospheric Sciences and Climate (ISAC) CNR, Italy
[3] CIMA Research Foundation, Italy
[4] Research Institute for Geo-Hydrological Protection (IRPI) CNR, Italy;
[5] European Centre for Medium-Range Weather Forecasts, Reading, United Kingdom;

1 Synoptic analysis

A low pressure area, centred over the Strait of Sicily, lead to disturbed weather conditions on the two main Italian islands and on the southernmost regions of the peninsula, especially on the Ionian sectors of Calabria, with winds from the east becoming strong. On October 25th, 2021 bad weather affects the southern regions, with more intense and persistent phenomena in Calabria, where the easterly winds are very strong. On 26th the low pressure is still present in the Ionian area, with widespread rain and thunderstorms once again over the eastern areas of Sicily and Calabria.

On October 25th, 2021 an intense Mediterranean Cyclone develops over the Sea south of Sicily. In the Balkan area, a strong high-pressure system is stationary, effectively blocking the movement of the low-pressure system (Figure 1 and Figure 2). The analysis in high atmospheric layers reveals clearly that a split of the
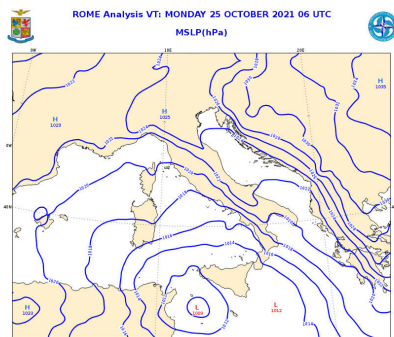

Figure 1. OCTOBER 25 at 06:00 UTC MSLP Mean sea level pressure analysis. Source Meteo Am.
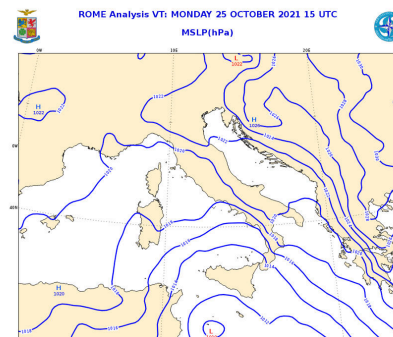
Figure 2. 25 OCTOBER at 15:00 UTC MSLP Mean sea level pressure analysis. Source Meteo Am.

polar Jet forces the Mediterranean Cyclone development over North Africa and

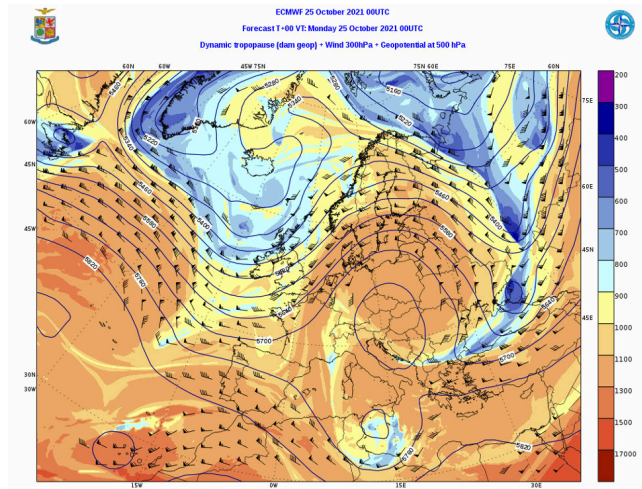Sicily. Note the stratospheric air intrusion in the left region of the Jet, over the Libyan Sea Figure 3.

Figure 3. Dynamic tropopause, Wind in 300 hPa and Geopotential at 500 hPa, analysis ECMWF of 25 OCTOBER 2021 at 00 and 15 UTC. Source Meteo Am.

2   Antecedent Conditions

The soil moisture wetness index estimated by ASCAT is here reported in order to evaluate the antecedent condition. The Figure 4 and Figure 5 show the surface soil moisture conditions estimated the 24 of October, before the occurrence of the precipitation,
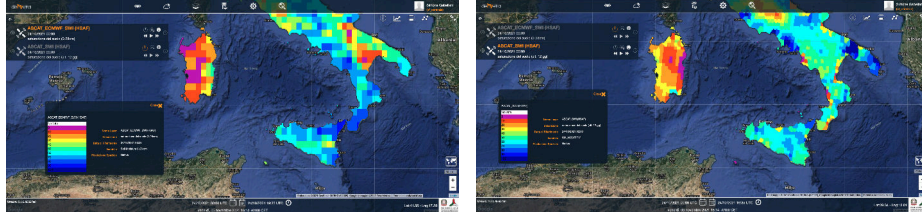

Figure 4. Surface Soil Moisture (HSAF, product derived from H14)

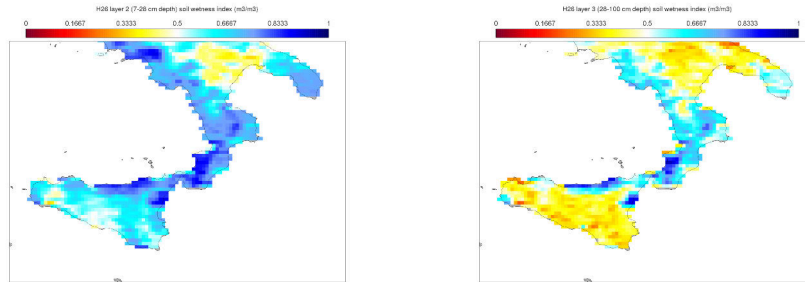**Figure 5.** Surface Soil Moisture (HSAF, product derived from H16)

Figure 6. Layer 2 (28-100 cm) soil moisture (HSAF, product derived from H26) on 24th October 00 UTC

Figure 7. Layer 3 (28-100 cm) soil moisture (HSAF, product derived from H26) on 24th October 00 UTC

respectively by H SAF SM-DAS-2 and SSM-ASCAT- NRT-soil moisture products.

Both products indicate wet conditions in the area where there was flooding, as reported in Figure 8. To assess the cause of the flooding, it is also useful to look at the root-zone soil moisture (RZSM) conditions. Figure shows the soil wetness index for the new 10 km resolution RZSM-ASCAT-NRT-10km product, called H26, on the 24th October for layer 2 (7-28 cm depth) (left) and layer 3 (28-100 cm depth) (right) at 00 UTC. Evidently the RZSM conditions are close to saturation in the affected regions.
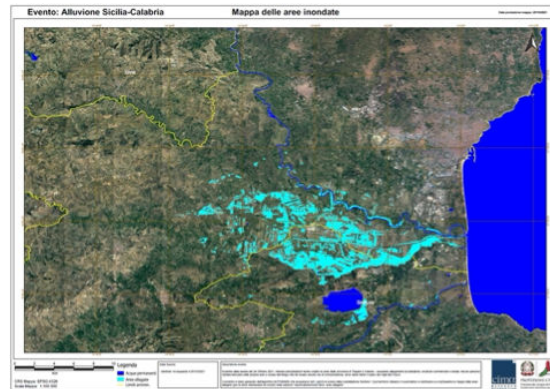
Figure 8. Flooded areas

The soil moisture estimated by H SAF Soil Moisture products is consistent also with the FloodPROOFS (Figure 9) (Bruno et al., 2021), even if FloodPROOFS shows a more saturated soil than the satellite products (Figure 4 and Figure 5). This is probably because FloodPROOFS has integrated more recent precipitation observations. The forecasting chain includes the distributed hydrological model Continuum (Silvestro et al., 2013) and allows to monitor the spatial and temporal evolution of the event. In particular the "return period product" identify the most severely affected areas.
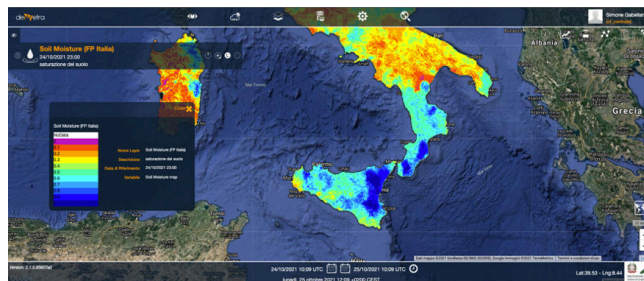

Figure 9. OCTOBER 24: Soil moisture - (Soil Moisture modelled by FP - spatial resolution 500m)

3   Ground data

Figure 10 represents accumulated rainfall over the whole period from 24 October 2021 at 00:00 UTC to 29 October 2021 at 23:55 UTC, showing the large amount of precipitation occurred on southern Italy during the pinpointed event.
In Figure 11 the product of merging between DPC radar and rain gauges, which shows the accumulated rainfall at the same time of Figure 10, is given.
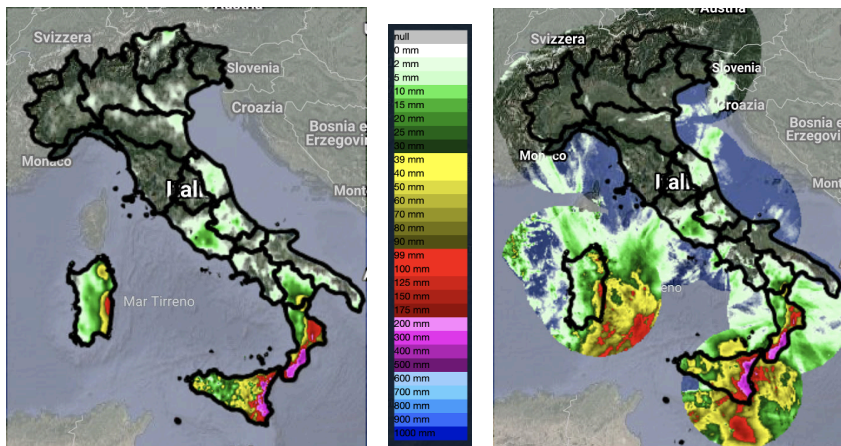

Figure 10. Rain map - accumulated rainfall over the whole period from 24 October 2021 at 00:00 UTC to 29 October 2021 at 23:55 UTC

Figure 11. Merging DPC radar+rain gauges - accumulated rainfall at the same time of Figure 10
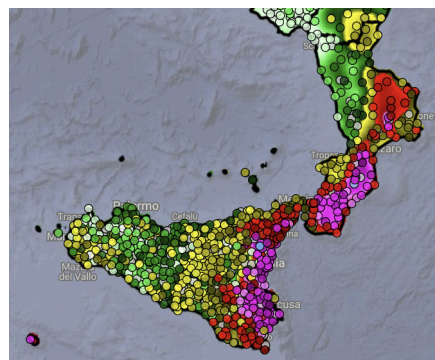

Figure 12. Rain map and rain gauges - accumulated rainfall over the whole period from 24 October 2021 at 00:00 UTC to 29 October 2021 at 23:55 UTC

Figure 12 shows accumulated rainfall, over the whole period from 24 October 2021 at 00:00 UTC to 29 October 2021 at 23:55 UTC, focusing on the most affected area.
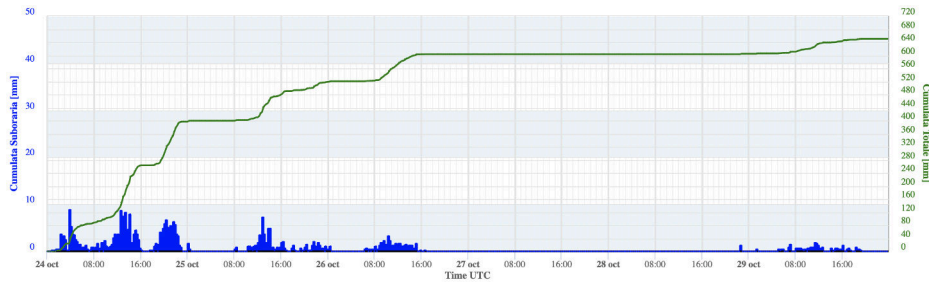In Figure 13 the Etna rain gauge pattern output is given for the same period.

Figure 13. Etna rain gauge output

4   Monitoring

4.1   Satellite products

The event has been continuously monitored by satellite acquisitions that provided data and products of a very wide variety of types: precipitation, cloud altitude, cloud types, soil moisture, flooded areas and many others.

The Meteosat satellite is particularly useful for observing and monitoring weather events. As shown in Figure 14, with the IR channels of the MSG it is possible to follow the evolution and trajectory of the Cyclone every 15 minutes. The figure shows for each of the 6 days ranging from 25 to 30 October an acquisition of the IR channel at 10.8 microns with the position of the center of the cyclone highlighted with a red circle. In the early hours of 25 October (a), the Cyclone formed close to the coasts of North Africa and continued its trajectory (b) towards the east/south-east until 27 October (c). On 28 October (d) it strengthened and moved closer to Sicily, reaching its closest point to Italy on 29 October (e). Finally, from 30 October (f) it has definitively moved south-east towards the coasts of Libya. The H SAF consortium (supported by EUMETSAT) provides
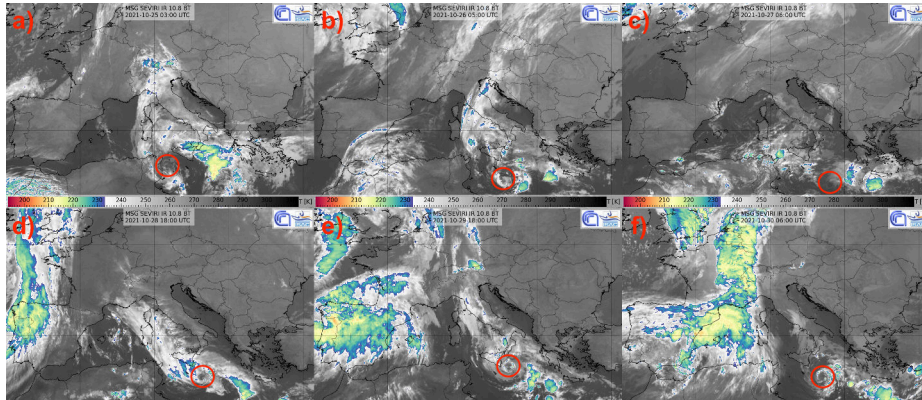

Figure 14. MSG IR 10.8 micron acquisitions from 25ft to 30th October 2021. Red circle highlights the centre of the Cyclone for each day.

satellite-based products for hydrology purposes. In particular, the estimation of surface precipitation is one of the objectives pursued by the project and perhaps represents the most stimulating challenge.

Instantaneous precipitation rate as well as temporally accumulated (hourly up to 24-hourly) precipitation is estimated both from passive microwave (PMW) measurements from Low Earth Orbit (LEO) satellites and from IR data from geostationary (GEO) satellites Mugnai et al. (2013). The products that more than others allowed us to follow the evolution of the event are those based on the SEVIRI sensor on board the MSG, namely, P-IN-SEVIRI-PMW (H60) (instantaneous) and P-AC-SEVIRI-PMW (accumulated) (H61). Both exploit the

precipitation rate estimates derived from PMW sensors and the MW/IR blended rapid-update technique, and provide the instantaneous precipitation rate every 15 minutes (H60) and the hourly and daily accumulated precipitation (H61).

As shown in Figure 13 the event has involved Sicily mainly in five days: on 24th, 25ft, 26th, 28th and 29th October. In this section, the role of satellite data for monitoring purposes during the days which have mainly affected the southernmost part of Italy is discussed.

24th October, 2021 Figure 15 shows the first moments of the beginning of the event that involved Sicily, as observed by H60 product. The estimated precipitation on the island was intense, particularly on the eastern coast, with maximum precipitation rate values over 40 mm/h. Off the African coast it was possible to observe the first signs of a clear trend towards a cyclonic rotation, a fundamental characteristic during the formation and before the intensification of the cyclone itself. The hourly precipitation starting from the 4 steps shown above
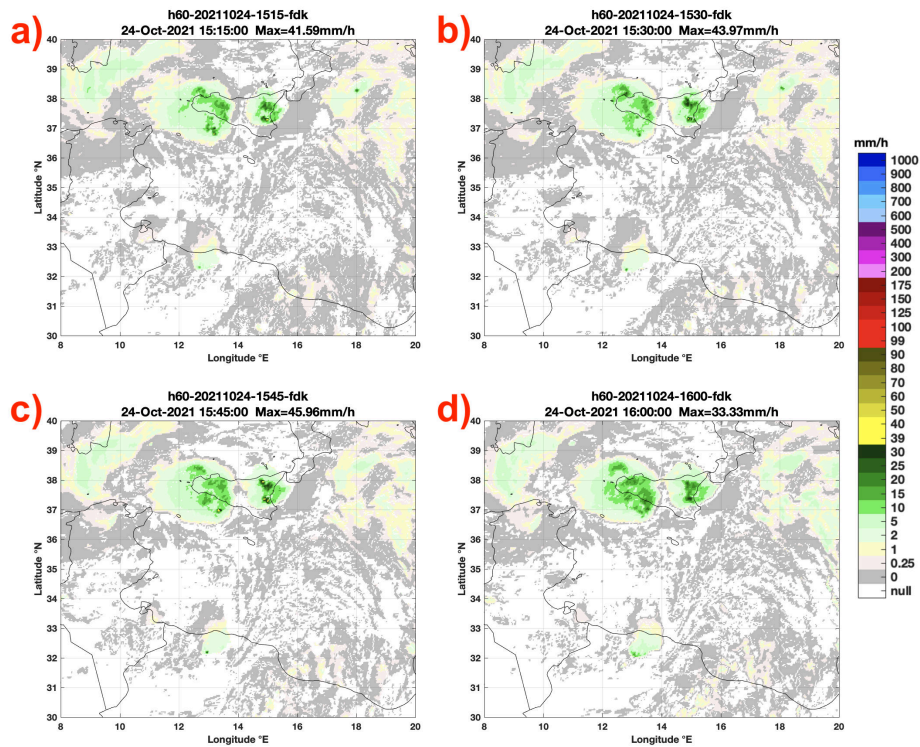

Figure 15. 24 Oct., 2021 15:15 - 16:00UTC: Instantaneous precipitation estimated by P-IN-SEVIRI-PMW (H60) in four subsequent steps: at 15:15UTC (a), at 15:30UTC (b), at 15:45UTC (c) and at 16:00UTC (d).

was produced by H61 product and shown in figure 16 on the left. On the right, instead, the interpolated rain gauge data is shown, which represents the ground reference. It is possible to observe that the precipitation products follow the precipitation pattern well, identifying two distinct areas of precipitation on Sicily. On the west side, the intensities were low-medium with values around 10 mm in agreement with ground observations.

The eastern part had more intense precipitation values, with peaks estimated by satellite up to 24mm distributed over two positions. Similarly, the raingauge observations identified two precipitation peaks along the east coast, with values equal to 28 and 40mm, respectively.
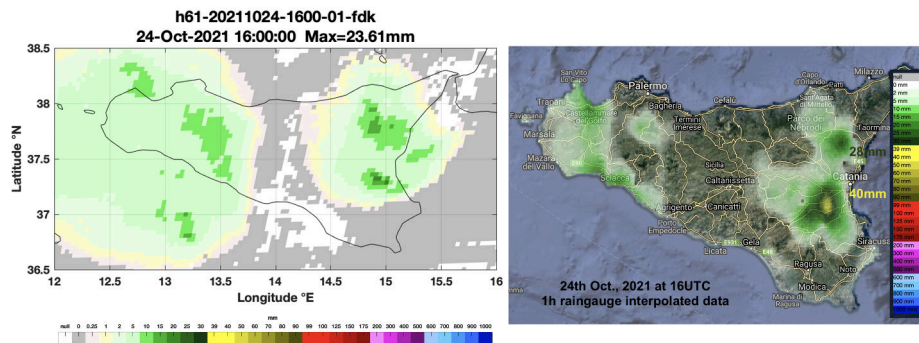

Figure 16. 24 Oct., 2021 16:00 UTC: 1h accumulated precipitation estimated by P-AC-SEVIRI-PMW (H61) on the left and the correspondent rain gauges measurements interpolated on the right.

25th October, 2021 In Figure 17 the comparison between two satellite precipitation rate products, one from MSG SEVIRI IR acquisitions on the left (MW/IR product P-IN-SEVIRI-PMW, H60), and one by the SSMIS acquisition on board DMSP17 satellite on the right (PMW product P-IN-SSMIS, H01, Casella et al. (2013)), around at 06:15UTC of 25 Oct., 2021 is shown. Observing the SEVIRI acquisition it is evident, at south of Sicily, the presence of the characteristic hook shape (with very low precipitation) typical of cyclones and two main areas of precipitation: the first one as outpost to the rotation of the cyclone itself with values around 8 mm/h, the second one, much more extensive, on the Ionian Sea approaching Sicily and Calabria, with intense precipitation values exceeding 20 mm/h. On the right, it is possible to observe the same areas of precipitation above described but with greater detail in terms of intensity. In particular, near

Sicily there was a convective cell with medium-high intensity that produced the precipitation on subsequent hours of 25th October (80 mm), as shown in the Figure 13 of the Etna rain gauge.
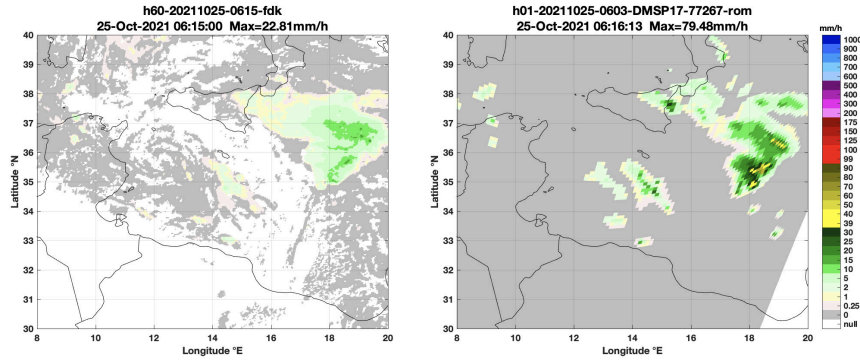

Figure 17. 25 Oct., 2021 at 06:15UTC: Instantaneous precipitation rate estimated by two H SAF products: P-IN-SEVIRI-PMW (H60) on the left, P-IN-SSMIS (H01 new rel.) on the right.

26th October, 2021 On 26th October, 2021, the cyclone shifted towards east, reaching 14°E longitude (and 35.5°N latitude). Observing H60 product in Figure 18 on the left, it is evident the center of the cyclone located 100 km at south of Sicily. Two main areas of precipitation are identified: the first one close to the center of rotation and the second more extensive in the Ionian Sea with more intense precipitation rate peaks. The comparison with the PMW product P-IN-ATMS (H18) from ATMS acquisition (Sanò et al. (2016)) highlights the same precipitation areas with slightly lower estimated values compared to H60. Note that the spatial resolution of ATMS is significantly lower than that of SE-VIRI). Figure 19 shows the accumulated precipitation from 24 to 26 October 2021 obtained by ground observations and 4 satellite products, namely 3 H SAF products (Level 3 MW-based daily precipitation (H-AUX-23) ((Ciabatta et al., 2017)), SM2RAIN ((Brocca et al., 2014) (Brocca et al., 2019)), and MW/IR H61), and one NASA GPM product MW/IR IMERG Early Run. Satellite products are consistent with ground observations clearly detecting areas with larger precipitation accumulation. Note that over Eastern Sicily, raingauges are missing and very likely the satellite derived precipitation accumulations are more reliable.

28th October, 2021 The GPM Core Observatory (GPM-CO) Dual-frequency Precipitation Radar (DPR) overpass of the Cyclone at 14:52 UTC allows to
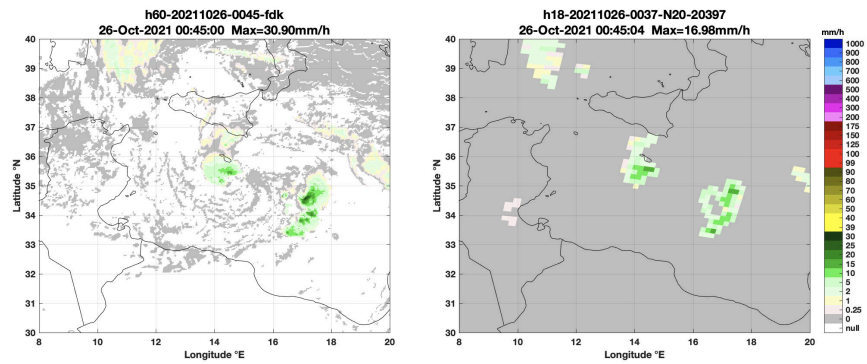
Figure 18. 26 Oct., 2021 at 00:45UTC: Instantaneous precipitation estimated by two H SAF products: P-IN-SEVIRI-PMW (H60) on the left, P-IN-ATMS (H18) on the right.
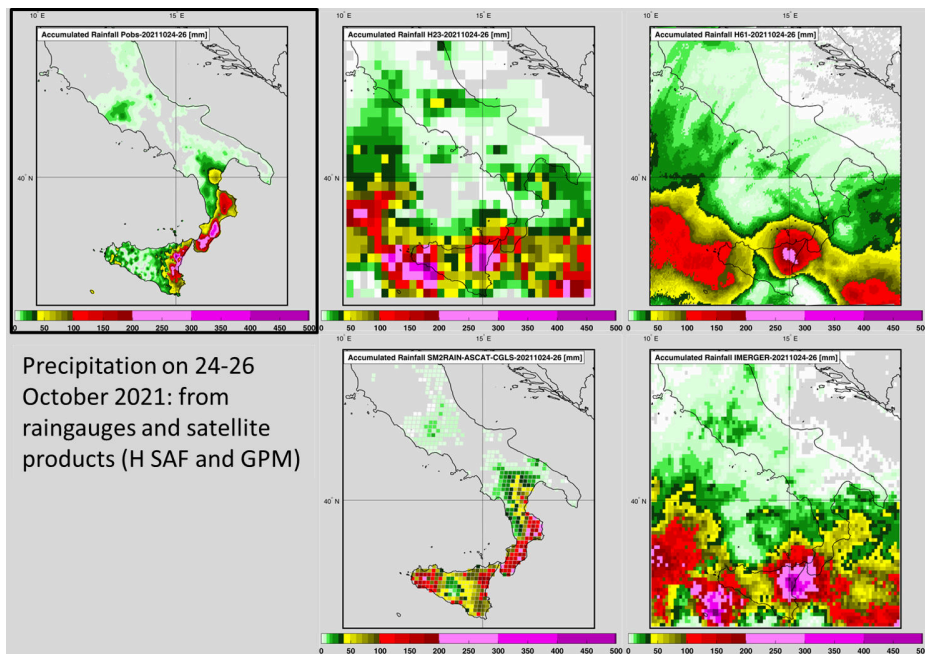

Figure 19. Accumulated precipitation from 24 to 26 October 2021 obtained by ground observations and by 4 satellite products: H SAF Level 3 MW-based daily precipitation (H-AUX-23), SM2RAIN, H SAF MW/IR H61, and NASA GPM MW/IR IMERG Early Run).

study different microphysical and dynamical characteristics. GPM-CO orbit intersected the center of the cyclone at 16.5°E, 35.5°N at 14:52 UTC as shown in

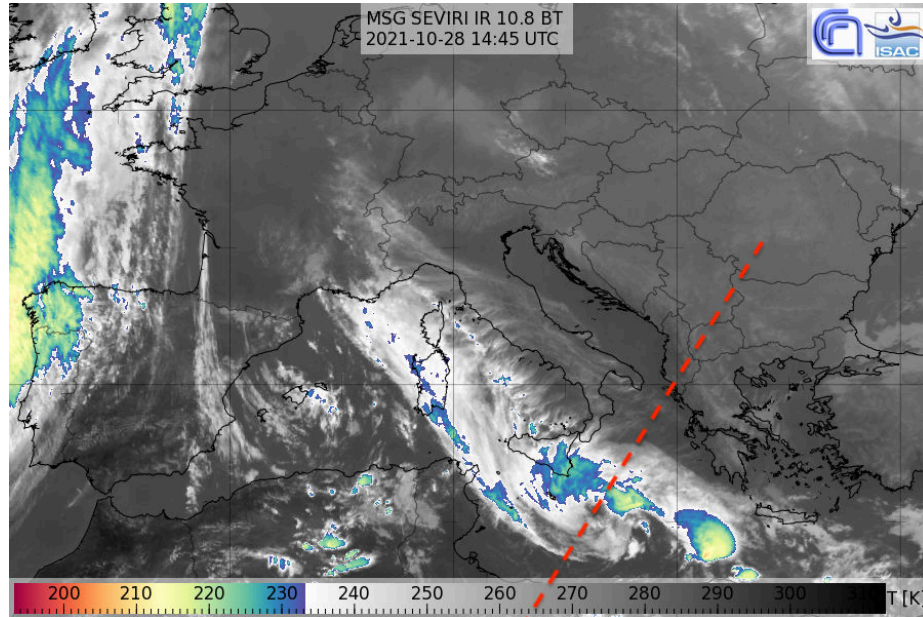Figure 20. Reflectivity measurements, provided by the DPR at Ku and Ka band,

Figure 20. 28th Oct., 2021: GPM trajectory (14:52UTC) overlapped on the MSG acquisition by IR 10.8 micron at 14:45UTC.

allow for example to estimate the precipitation rate (Figure 21) with a high spatial resolution (5km) and also to estimate the height of the precipitating clouds (Figure 22). It is interesting to note that the deeper clouds in the north-eastern sector of the cyclone are associated to very light surface precipitation according to DPR (below 1 mm/h), while the low level clouds, which characterize most of the cyclone rainbands, are associated to light to moderate precipitation rate.

Instantaneous precipitation rate estimates by H60 at 15 UTC and by H SAF PMW auxiliary module H-AUX-20 (P-IN-GMI) ((Sanò et al., 2018)) from GPM Microwave Imager (GMI) acquisition at 14:52 UTC are shown respectively in Figure 23 and 24. The PMW product show very light precipitation (below 1-2 mm/h) in most of the shallow rain bands, reproducing the DPR precipitation pattern, except in correspondence with the deeper cloud in the north-eastern sector, where, as opposed to the DPR, moderate precipitation is observed. The presence of precipitation in this area is clearly evidenced by the GMI measurements. It is likely that the DPR surface rainfall rate estimates here are affected by attenuation and sensitivity issues,

29th October, 2021 29th October was the last day in which the southern Italian area was affected by this long lasting event. On this day, the Cyclone
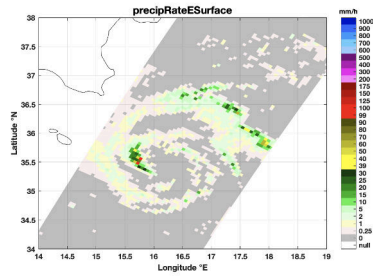
Figure 21. GPM Normal Scan acquisition mode: precipitation rate [mm/h] estimated at near-surface level on Oct. 28 14:52 UTC
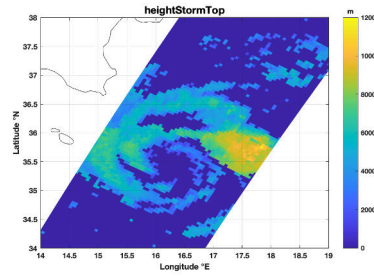

Figure 22. GPM Normal Scan acquisition mode: storm top height [m].
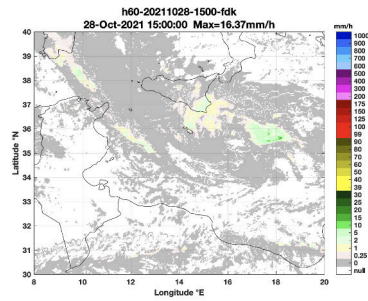

Figure 23. Instantaneous precipitation rate estimated by H60 product at 15UTC of 28th Oct., 2021.
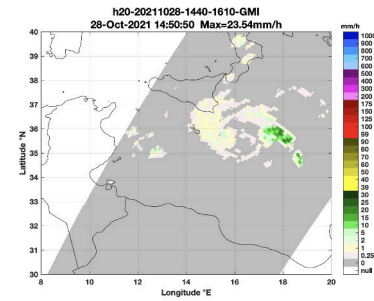

Figure 24. Instantaneous Precipitation rate product P-IN-GMI from GPM-CO GMI acquisition (H SAF Auxiliary module H_AUX-20)

center was at its closest position to Sicily, in position 16°E, 36.5°N as it is evident in the Figure 25. The precipitation estimated by satellite was arranged in two large bands: one in the northward branch and the other in the southward branch of the rotating cyclone. Both H SAF products shown in the figure (the MW/IR H60 and the PMW product from the AMSU/MHS acquisition P-IN-MHS, H02B, Sanò et al. (2016)) observe the same precipitation pattern and intensity (medium-low) with respect to the cyclone center.

In the following days, the cyclone tended to move to the south and headed further east on the Ionian Sea and towards the coasts of Libya.
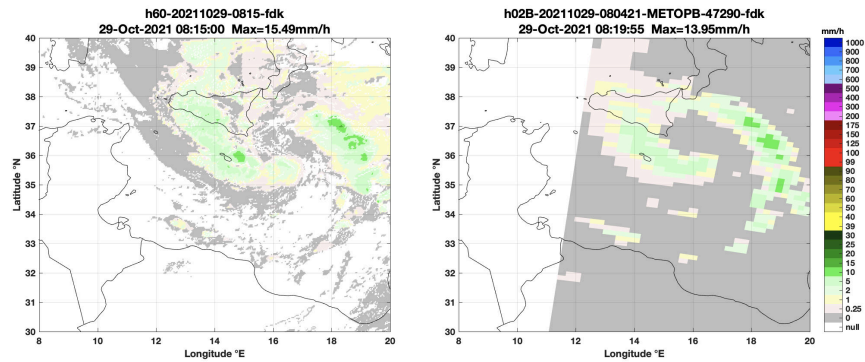

Figure 25. 29 Oct., 2021 at 08:19UTC: Instantaneous precipitation rate estimated by two H SAF products: P-IN-SEVIRI-PMW (H60) on the left, P-IN-MHS (H02B) on the right.

Links to Twitter's posts:
https://twitter.com/HydroSAF/status/1452662676618989575?s=20
https://twitter.com/hydrosaf/status/1452670034971557888?s=21
https://twitter.com/hydrosaf/status/1453271168765542409?s=21
https://twitter.com/hydrosaf/status/1453248093076561921?s=21

4.2   Models

The DPC national flood forecasting chain, FloodPROOFS (Bruno et al. 2021, https://www.mdpi.com/2073-4433/12/6/771), fed by the meteorological models COSMO5M and WRF showed severe hydrological conditions for Calabria and Sicilia. In Calabria, the forecast of 23, in almost all the modelled sections, provided for exceeding the maximum threshold (red threshold) (Figure 27 and 28). The FloodPROOFS include the hydrological model Continuum used for hydrovalidation in HSAF. The morning forecast of October 24 confirms possible critical issues in Calabria and add possible severe hydrological events in Sicily (Figures 29 and 30) in the province of Messina and Catania. The morning forecast of October 25 (Figure 29) highlights the persistence of critical situations (Figure 30) due to residual precipitation on saturated soil (Figure 9).

Figure 26. OCTOBER 22 at 09 UTC: FlooPROOFS forecast (COSMO 5M input), all the markers of the river section are white, this means that no exeedance are expected.

Figure 27. OCTOBER 23 at 09 UTC: FlooPROOFS forecast (COSMO 5M input), when the forecast discharge exceed the maximum threshold the marker of the section turn red.

Figure 28. OCTOBER 23 at 09 UTC: FloodPROOFS probabilistic forecast for Bonamico Creek at Casignana-SS106 (Calabria), the vertical blue line is the date of the run of the hydrological chain, after this date the forecasted meteorological variable are used to fed the hydrological model.
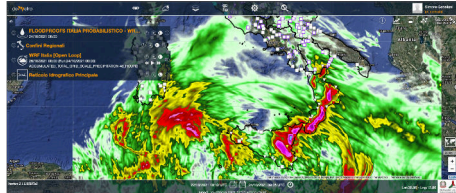
Figure 29. OCTOBER 24 at 09 UTC: WRF forecast (accumulated rainfall +48h).

Figure 30. OCTOBER 24 at 09 UTC: FlooPROOFS forecast (WRF input) - Expected exceedances: in addition to the sections in Calabria, there are sections in the provinces of Catania and Messina that turn red due to high discharge forecast.

Figure 31. OCTOBER 24 at 09 UTC: FloodPROOFS forecast (with COSMO 5M input) - Expected exceedances: almost all section in Calabria exceed the maximum treshold

Figure 32. OCTOBER 25 at 09 UTC: WRF forecast (cumulative +48h)

Figure 33. OCTOBER 25 at 09 UTC: Flood-PROOFS forecast (WRF input)

The analysis of soil moisture conditions, FloodPROOFS (Figure 9) shows a more saturated soil than the satellite products (Figure 4 and Figure 5) because it also integrates more recent precipitation observations. The forecasting chain
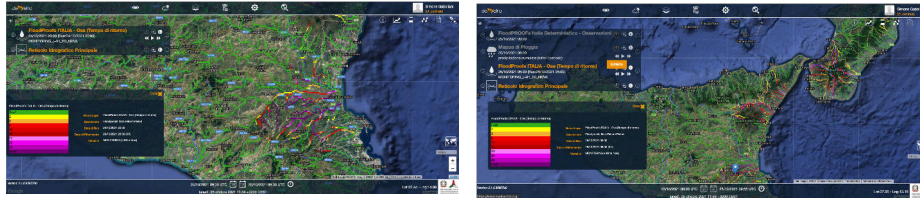
Figure 34. OCTOBER 25 at 09:30 UTC: FloodPROOFS - severity of the event expressed as return times of the discharge estimated according to model climatology. The modelling chain highlights the most severely affected areas - including Catania plain, Scordia and Ogliastro (Catania)

Figure 35. OCTOBER 25 at 09:30 UTC: FlooPROOFS - severity of the event expressed as return times of the discharge estimated according to model climatology - Modelling highlights the worst affected areas, including Messina and Reggio Calabria

Figure 36. OCTOBER 25 09 UTC: FloodPROOFS probabilistic forecast for Ancinale River at Satriano Marina (Calabria).

includes the distributed hydrological model Continuum (Silvestro et al. 2013) and allows to monitor the spatial and temporal evolution of the event. In particular the "return period product" identify the most severely affected areas. Figures 35 and 36 shows the return period of the discharge in each pixel of the modelled river network. The return periods are estimated using the climatology of the forecasting chain and can different from the official return periods of the basin authorities studies. They provide an index of severity of the event that is consistent within the modelling framework. The morning forecast of the Flood-PROOFS chain in October 26 (Figures 37 and 38) highlights the persistence of critical situations in south-Calabria and in Catania).

The heavy precipitation of the 26th severely hit the city of Catania (Figure 39) leading to intense discharge and heavily saturated soil (Figure 40).
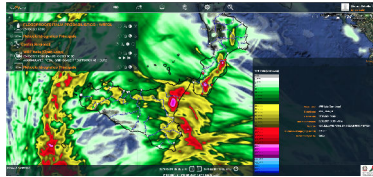
Figure 37. OCTOBER 26 09 UTC: WRF forecast (accumulated rainfall +48h).

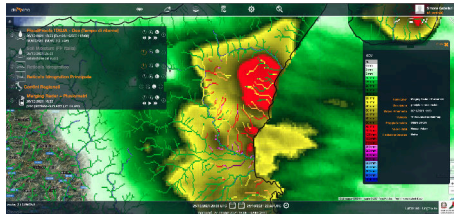**Figure 38.** OCTOBER 26 09 UTC: FloodPROOFS forecast (WRF input).

Figure 39. OCTOBER 26: Merging DPC radar+rain gauges - accumulated rainfall over the last 24 hours at 16:30 on 26 October 2021.
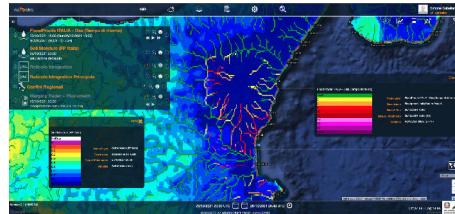

Figure 40. OCTOBER 26: Flood-PROOFS, severity of the event expressed as return times of the discharge, estimated according to model climatology, and modelled soil moisture map - Catania city severely affected.

References

Brocca Luca, Ciabatta Luca, Massari Christian, Moramarco Tommaso, Hahn Sebastian, Hasenauer Stefan, Kidd Richard, Dorigo Wouter, Wagner Wolfgang, Levizzani Vincenzo. Soil as a natural rain gauge: Estimating global rainfall from satellite soil moisture data // Journal of Geophysical Research: Atmospheres. 2014. 119, 9. 5128–5141.

Brocca Luca, Filippucci Paolo, Hahn Sebastian, Ciabatta Luca, Massari Christian, Camici Stefania, Schüller Lothar, Bojkov Bojan, Wagner Wolfgang. SM2RAIN–ASCAT (2007–2018): global daily satellite rainfall data from AS-CAT soil moisture observations // Earth System Science Data. 2019. 11, 4. 1583–1601.

Bruno Giulia, Pignone Flavio, Silvestro Francesco, Gabellani Simone, Schiavi Federico, Rebora Nicola, Giordano Pietro, Falzacappa Marco. Performing Hydrological Monitoring at a National Scale by Exploiting Rain-Gauge and Radar Networks: The Italian Case // Atmosphere. 2021. 12, 6. 771.

Casella D., Panegrossi G., Sanò P., Mugnai A., Smith E.A., Tripoli G.J., Dietrich S., Formenton M., Di Paola F., Leung H. W.-Y., Mehta A.V. Transitioning from CRD to CDRD in Bayesian retrieval of rainfall from satellite passive microwave measurements, Part 2: Overcoming database profile selection ambiguity by consideration of meteorological control on microphysics // IEEE Trans. Geosci. Remote Sens. 2013. 51, 9. 4650–4671.

Ciabatta L., C. Marra A., G. Panegrossi, D. Casella, P. Sanò, S. Dietrich, C. Massari, L. Brocca. Transitioning from CRD to CDRD in Bayesian retrieval of rainfall from satellite passive microwave measurements, Part 2: Overcoming database profile selection ambiguity by consideration of meteorological control on microphysics // J. of Hydrology. 2017. 545. 436–450.

Mugnai A., Casella D., Cattani E., Dietrich S., Laviola S., Levizzani V., Panegrossi G., Sanò P., Biron D., De Leonibus L., Melfi D., Rosci P., Vocino A., Zauli F., Puca S., Rinollo A., Milani L., Porcù F., Gattari F. Precipitation products from the Hydrology SAF // Nat. Hazards Earth Syst. Sci. 2013. 13. 1959–1981.

Sanò P., Panegrossi G., Casella D., Marra A. C., Di Paola F., Dietrich S. The new Passive microwave Neural network Precipitation Retrieval (PNPR) algorithm for the cross-track scanning ATMS radiometer: description and verification study over Europe and Africa using GPM and TRMM spaceborne radars // Atmos. Meas. Tech. 2016. 9. 5441–5460.

Sanò P., Panegrossi G., Casella D., Marra A. C., D'Adderio L. P., Rysman J.-F., Dietrich S. The Passive Microwave Neural Network Precipitation Retrieval (PNPR) algorithm for the Conical Scanning GMI Radiometer // Remote Sens. 2018. 10. 1122.

Silvestro Francesco, Gabellani S, Delogu F, Rudari R, Boni G. Exploiting remote sensing land surface temperature in distributed hydrological modelling: the

example of the Continuum model // Hydrology and Earth System Sciences. 2013. 17, 1. 39–62.